

Hydrothermal alteration in association with large impact basins on Mars

Christina E. Viviano (1) and Michael S. Phillips (2)

(1) Johns Hopkins University Applied Physics Laboratory, Laurel, MD (christina.viviano@jhuapl.edu)

(2) The University of Tennessee, Knoxville, TN

Abstract

Detailed mapping of CRISM targeted and mapping data across the region between Isidis and Hellas Basins reveal diverse metamorphic and hydrothermal alteration products that may be the result of processes related to basin impact formation.

1. Introduction

The area west of Isidis Basin (Nili Fossae) exposes a region diverse in alteration mineralogy composition, including phyllosilicates and other silicates indicative of metamorphic alteration across the region. The underlying low-Ca pyroxene bearing basement unit in the Nili Fossae region has experienced varied metamorphism, resulting in metamorphic grades from diagenesis to prehnite-pumpellyite facies (and perhaps greenschist facies) [1-3]. An overlying olivine-bearing unit in the easternmost portions of Nili Fossae (along the western Isidis rim) reveals differing alteration products including serpentine, magnesium carbonate [4], and a spectrally unique Mg-bearing phyllosilicate, possibly consistent with talc [2,5]. One interpretation of the association of these products is that they are evidence for hydrothermal alteration of the olivine-rich protolith, from the formation of talc and carbonate through the carbonation of serpentine [2,5].

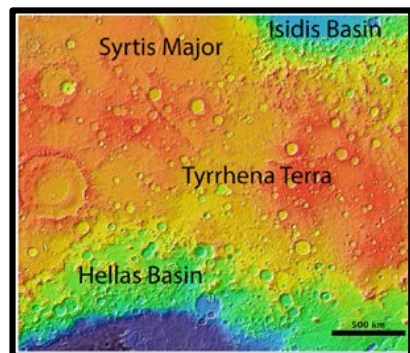


Figure 1. MOLA elevation map of study region.

2. Methods

Here we analyze CRISM targeted and mapping data for the presence of metamorphic- and hydrothermally-related alteration phases in the greater Tyrrhena Terra region between Isidis and Hellas Basins (Fig. 1), where past studies indicate similar assemblages may be present [6,7]. Several hundred new prototype MTRDR calibrated images [8] (through 06/2008) and updated spectral parameters [9] were analyzed within this region to allow for more complete mapping of phases. Multispectral mapping data across this region are also used to map and examine the distribution of alteration (metamorphic vs. hydrothermal) and determine potential associations with Isidis and Hellas basins.

3. Results

Initial mapping efforts of the primary lithology reveals significant plagioclase abundance in the northern Hellas Rim [10], even more extensive than initially identified by [11]. Low-Ca pyroxene (LCP) dominates the Noachian-aged crustal materials between Hellas and Isidis, whereas high-Ca pyroxene (HCP) appears more often associated with younger volcanic provinces (e.g., Syrtis Major) and sands that may not be locally derived. Alteration phases, including Mg-smectite, chlorite/prehnite, hydrated silica, kaolinite, illite/muscovite, analcime and other zeolites, Mg-carbonate, and possible talc, appear throughout the region. At a minimum, low temperature diagenetic to zeolite-facies metamorphic grade, indicated by the presence of illite and chlorite (the transformation of trioctahedral smectites to chlorites and dioctahedral smectites to illites during diagenesis) and zeolite (including analcime), is prevalent throughout Tyrrhena Terra. Prehnite, which forms at 200-400°C, provides clear evidence for higher temperature alteration (prehnite-pumpellyite facies [e.g., 1]) and appears only in the region

between two basins in mapping thus far. Carbonate, possible talc, and kaolinite appear to be associated with the southern rim of Isidis Basin (and western rim near Nili Fossae [2]) and the northern rim of Hellas Basin (Fig. 2). There is also a region surrounding Oenotria Scopuli, a basin-ring structure [12] circumferential to Isidis (black dashed line, Fig. 2), where carbonate is identified [7]. Kaolinite and possible talc are also observed near this scarp.

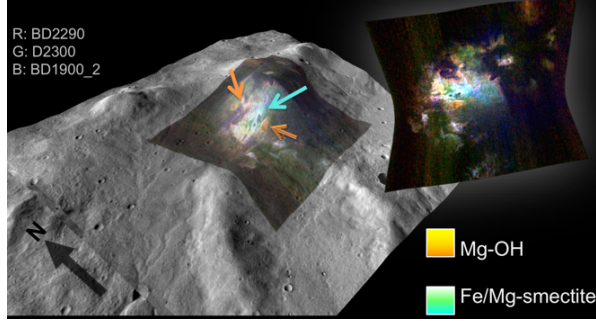


Figure 2. CRISM image FRT00008144 summary parameter RGB composite [2] used to discriminate Fe- vs. Mg-bearing phyllosilicates overlain on CTX imagery. Data are draped on HRSC topography data with vertical exaggeration.

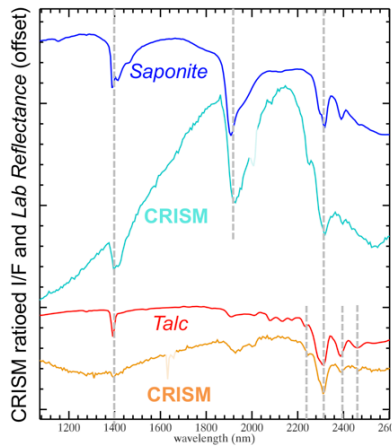


Figure 3. Extracted CRISM spectra (from arrows in Fig. 2) as compared to laboratory spectra of Mg-bearing phyllosilicate species.

Particularly along the northern rim of Hellas, we observe an Mg-OH spectral component. The CRISM spectra have distinctly little to no spectral features due to bound water (lack of deep 1.4- and 1.9- μm bands; Fig. 3, bottom). The material displays strong 2.31- and 2.39- μm bands and shallow, but present \sim 2.25- μm band and narrow 1.39- μm band. The \sim 1.4- μm band depth is commonly weak in Fe/Mg-

phyllosilicates on Mars and may be due to effects of mixing with other opaque Fe-bearing oxides [e.g., 1]. More hydrated Mg-phyllosilicate phases consistent with Mg-smectite (Fig. 3, top) is present throughout the region, though chlorite dominates in the region between the two basins.

4. Discussion and Conclusions

Although the talc-related spectral component appears related to plagioclase-bearing knobs, it is more likely derived from an Mg-rich pyroxene/olivine lithology that co-occurs with these features [10]. The apparent association of plagioclase-rich material, potentially emplaced as anorthositic plutons [11], and talc (+/-carbonate) may suggest a metasomatic origin for the talc via contact metamorphism of an Mg-rich ultramafic unit during intrusion of the anorthositic pluton. Variability in metamorphic grade will be tested for any spatial trends associated with proximity to the basins, and may be revealed with the completion of the mapping effort.

Acknowledgements

This work was completed with the support of NASA MDAP grant number NNX14AM16G.

References

- [1] Ehlmann et al. (2009) JGR, 114.
- [2] Viviano et al. (2013) JGR, 118, 1858-1872.
- [3] Carter et al. (2013) Planet. Space Sci., 76, 53-67.
- [4] Ehlmann et al. (2008) Science, 322, 1828-1831.
- [5] Brown et al. (2010) EPSL, 297, 174-182.
- [6] Fraeman et al. (2009) LPSC, #2320.
- [7] Bultel et al. (2015) Icarus, 260, 141-160.
- [8] Seelos et al. (2012) Planet. Data Workshop, USGS, VA.
- [9] Viviano-Beck et al. (2014) JGR, 119, 1403-1431.
- [10] Phillips et al. (2018) 1st Gy: Differentiation, #4026.
- [11] Carter & Poulet (2013) Nat. Geo., 6, 1008-1012.
- [12] Tanaka et al. (2013) USGS, 3292.